Int. J. Plant Bas. Pharm. 1(1), 56-64

INTERNATIONAL JOURNAL OF PLANT BASED PHARMACEUTICALS

https://ijpbp.com

RESEARCH ARTICLE

OPEN ACCESS

Assessment of apigenin-7-glucoside and luteolin-7-glucoside as multi-targeted agents against Alzheimer's disease: a molecular docking study

Erman Salih Istifli [a,*], Cengiz Sarikurkcu [b]

[a] *Cukurova University, Faculty of Science and Literature, Department of Biology, TR-01330, Adana-Turkey*
[b] *Afyonkarahisar Health Sciences University, Faculty of Pharmacy, Department of Analytical Chemistry, TR-01330, Afyonkarahisar-Turkey*

ARTICLE INFO

Article History:

Received: 31 July 2021
Revised: 06 August 2021
Accepted: 10 August 2021
Available online: 10 August 2021

Edited by: B. Tepe

Keywords:
Alzheimer's disease
AChE
BChE
Amyloid precursor protein
β-amyloid peptide
Molecular docking

ABSTRACT

Although the incidence of Alzheimer's disease (AD) is increasing in society, unfortunately, no definite progress has been made in treating this disease yet. In this study, the potential of apigenin-7-glucoside (A7G) and luteolin-7-glucoside (L7G) to be used as multi-targeted agents in AD was investigated by molecular docking calculations against the acetylcholinesterase (AChE), butyrylcholinesterase (BChE), amyloid precursor protein (APP) and 42-residue beta-amyloid peptide (Aβ). A7G and L7G exhibited very high binding affinity (-9.42 and -9.60 kcal/mol for A7G; -9.30 and -9.90 kcal/mol for L7G) to AChE and BChE, respectively, while the affinities of these two flavonoid glycosides towards APP and Aβ peptide (-6.10 and -6.0 kcal/mol for A7G; -6.30 and -6.10 kcal/mol for L7G) were moderately strong. Compared to rivastigmine, A7G and L7G exhibited a highly significant binding affinity, even stronger than rivastigmine, for AChE and BChE. Although A7G showed a more drug-like physicochemical character than L7G, both ligands were within the normal range for ADMET and did not show high affinity for cellular proteins, according to the results of SwissTarget analysis. According to the STITCH interaction analysis, both ligands had the potential to inhibit enzymes predominantly in the inflammatory pathway (ADIPOQ, NOS1, NOS2 and NOS3). As a result, A7G and L7G exhibit multi-targeted agent properties in AD. Our results should also be verified by experimental enzyme inhibition studies, which may be performed simultaneously on AChE, BChE, APP, and Aβ peptides.

1. Introduction

Dementia is a clinical syndrome that manifests itself with a series of symptoms and signs as memory, language disorders, psychological and psychiatric abnormalities, and damage to some activities in daily life (Burns and Iliffe, 2009). The most common form of dementia in the elderly population is Alzheimer's disease (AD), and the frequency of this disease increases with age (Ferri et al., 2005).

According to the cholinergic hypothesis, the oldest hypothesis about AD, the disease occurs due to decreased synthesis of the neurotransmitter acetylcholine (Francis et al., 1999).

* Corresponding author:
E-mail address: ermansalih@gmail.com (E. S. Istifli)
E-ISSN: 2791-7509
doi: https://doi.org/10.62313/ijpbp.2021.7

The two main enzymes responsible for this reduced acetylcholine in the brain are acetylcholinesterase (AChE) and butyrylcholinesterase (BChE). In healthy brain tissue, AChE and BChE function together and coordinate cholinergic neurotransmission via hydrolysis of ACh (Li et al., 2000). However, while BChE activity increases in AD patients, AChE activity remains unchanged or decreases (Greig et al., 2002). In addition to these known cholinergic functions of both enzymes, their non-cholinergic functions determined in the pathology of AD have started to emerge in recent years. In addition to its role in cholinergic synapses, it has been reported that AChE accelerates the formation of amyloid-beta-peptide (Aβ) and may play a role in the amyloid deposition in the brain of AD patients (Álvarez Rojas et al., 1996). In addition, biochemical studies have shown that AChE induces amyloid fibril formation and forms highly toxic AChE-Aβ complexes (Carvajal and Inestrosa, 2011; Dinamarca et al., 2010; Inestrosa et al., 2005). In addition, similar to AChE, BChE has also been reported to be associated with Aβ subpopulations and may play a role in plaque maturation observed in AD disease

Please cite this article as: Istifli, E.S., Sarikurkcu, C., 2021. Assessment of apigenin-7-glucoside and luteolin-7-glucoside as multi-targeted agents against Alzheimer's disease: a molecular docking study. International Journal of Plant Based Pharmaceuticals, 1(1), 56-64, https://doi.org/10.62313/ijpbp.2021.7.

(Darvesh et al., 2012). Thus, due to their altered roles in AD disease, both enzymes exhibit functional therapeutic target properties, and inhibition of these enzymes may be advantageous in ameliorating cholinergic function and blocking Aβ fibril formation in affected individuals.

Another hypothesis valid in the etiology of AD and has been put forward more recently is the amyloid hypothesis, which postulates that the extracellular Aβ peptide deposits in the brain tissue are the leading cause of the disease (Hardy and Allsop, 1991). The source of these neurotoxic Aβ peptides is the amyloid precursor protein (APP) a type-1 transmembrane glycoprotein that plays a significant role in the pathogenesis of AD (Spoerri et al., 2012). APP undergoes two different types of proteolytic processing, and the proteolytic pathway associated with AD is the amyloidogenic pathway. In this pathway, APP is first cleaved from the β-site, resulting in the sAPPβ ectodomain and the membrane-bound C-terminal domain (C99) (Gabuzda et al., 1994; Seubert et al., 1993). C99 can be enzymatically processed by γ-secretase, resulting in Aβ and the intracellular APP domain (Anderson et al., 1992).
Interestingly, the amyloidogenic process of APP occurs under physiological conditions, and thus imbalances in the amyloidogenic pathway are closely associated with the pathology of AD (Haass et al., 1992; Seubert et al., 1992). It has been reported that co-mutation of His149 and His151 residues localized in the N-terminal APP copper-binding domain (CuBD), which plays a role in APP maturation, to asparagine reduces the proteolytic processing of APP and that the CuBD domain may be a potential target of novel drugs in AD treatment (Spoerri et al., 2012). In addition, direct evidence has been reported that Aβ, the distinct hallmark of AD, is an activator of gradual damaging events induced in brain tissue by the aggregation of P-Tau (Sun et al., 2015).

Flavonoids are plant-based phytochemicals present in almost all plants found on earth, and as a result, they are consumed by humans through diet. Evidence obtained in recent years suggests that various flavonoids have positive effects on dementia and AD and reports that they positively affect neurocognitive performance (Airoldi et al., 2018). In addition, recent studies showed that flavonoid glycosylation was associated with a modest increase in the inhibitory activity (affinity) of these phytochemicals on various AD-causing proteins (Ali et al., 2019; Guzzi et al., 2017). In this context, the chronic treatment of apigenin 7-glucoside (A7G) was reported to ameliorate cognitive deficits in aged and LPS-intoxicated mice (Patil et al., 2003), while luteolin 7-O-β-d-glucoside (luteolin 7-glucoside) (L7G) significantly inhibited BChE and AChE activity in silico and in vitro studies (Uddin et al., 2020).

This study aimed to evaluate the inhibitory potentials of A7G and L7G, the flavonoid glycosides, against AChE, BChE, APP, and Aβ, which have direct roles in AD pathology using a molecular docking method. There has been no definitive treatment for AD, and current therapies only act to slow the course of the symptoms. A multi-target-inhibition approach could be rational in treating multifactorial AD, and such studies are scarce in the literature. Therefore, the development of a low side effect hit molecule(s) capable of inhibiting AChE, BChE, APP, and Aβ in a combined manner would have the potential to revolutionize the treatment of AD.

2. Materials and methods

2.1. Protein and ligand preparation

Molecular docking is a frequently used computational method for calculating the affinity of small molecules to their respective receptors, predicting their most favorable binding modes, and studying their mutual interactions within specific binding pockets of these receptors. The resolved crystal structures of recombinant human acetylcholinesterase (AChE) (PDB ID: 4EY6), human butyrylcholinesterase (BChE) (PDB ID: 4BDS), amyloid precursor protein copper-binding domain (APP) (PDB ID: 2FK1), and 42-residue beta-amyloid fibril (Aβ) (PDB ID: 2MXU) were retrieved from Protein Data Bank (PDB) with resolutions of 2.40 Å, 2.10 Å, 1.60 Å, respectively. However, the resolution information of 42-residue beta-amyloid fibril (PDB ID: 2MXU) was not available. Heteroatoms such as water molecules, co-crystallized inhibitors, and non-interacting ions on all proteins and Aβ fibril were removed, and missing atoms on amino acid residues were added with the 'Repair Missing Residues' tool of the AutoDockTools interface. Protonation states of ionizable side chains were assigned using the PropKa module of Vega ZZ (Li et al., 2005).

The 3D conformers of A7G and L7G (Figure 1) simulated in this study were retrieved from the PubChem database in .sdf format. The energy minimization of both ligands was performed using the universal force field (UFF) implemented in the Avogadro software (Hanwell et al., 2012). Then, the geometrically optimized ligand files were converted to .pdbqt format using the Open Babel open-source chemistry toolbox for further use in molecular docking simulations (O'Boyle et al., 2011). Rivastigmine, which was used as a positive control of AChE and BChE, was prepared for molecular docking simulations using the same processes as the other two ligands after being separated from the complex downloaded as PBD ID: 6EUE from the Protein Data Bank.

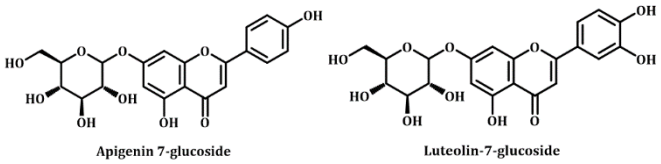

Figure 1. Chemical structures of A7G and L7G

2.2. Molecular docking

AMDock (https://github.com/Valdes-Tresanco-MS/AMDock-win) assisted molecular docking tool with AutoDock Vina was implemented in molecular docking of A7G, L7G, and rivastigmine into the defined catalytic sites of the AChE, BChE, APP, and Aβ (Trott and Olson, 2010; Valdes-Tresanco et al., 2020). The grid box coordinates were set to allow the ligands to interact with these target proteins' catalytic amino acid residues. In this context, we thought that it would be helpful to give brief information on the active regions of the APP and the Aβ: The copper-binding domain (His147, His149, and His151) of APP has been identified as the active site since this region has been reported to be important in APP folding and stability (Spoerri et al., 2012). In addition, the key residues His14, Glu22, Asp23, Gly33, Gly37, and Gly38 were selected as the active site of Aβ peptides since the side chains of these amino acids play a prominent role in the formation of amyloid fibrils (Hsu et al., 2018).

Prior to docking, the grid boxes of AChE, BChE, APP and Aβ were adjusted as follows: a) 82×56×54Å points (x: 15.71, y: 7.75, z: 49.32) for AChE; b) 70×62×54Å points (x: 139.93, y: 115.80, z: 41.74) for BChE; c) 30×30×30 Å points (x: 10.30, y: 18.90, z: 8.30) for APP; and 40×40×40Å points (x: -24.30, y: 6.21, z: 11.14) for Aβ.
In the configuration settings prepared for docking, the exhaustiveness was set as '56', and the number of separate docking

runs (number of poses) was set as '20'. In separate docking analyses, all potential binding modes (conformations) of A7G, L7G, and rivastigmine were clustered and ranked based on binding free energies (ΔG˚; kcal/mol) of the ligands' conformations which showed the lowest binding free energy against AChE, BChE, APP, and Aβ. The best docking conformations of the three ligands against protein targets calculated by AMDock were visualized and analyzed using Discovery Studio Visualizer v16.

2.3. Drug-likeness, ADMET profile, and target prediction

The determination of drug-likeness, ADMET, and target profiles of promising hit compounds in structure-based drug design (SBDD) is essential to reduce their side effects on the target organism. In this study, SwissADME, pkCSM, and SwissTargetPrediction online tools were used to investigate such effects of A7G and L7G (Daina et al., 2019a; Pires et al., 2015).

2.4. Network pharmacology analysis

The one-drug/one-target approach in drug discovery has some deficiencies in terms of safety and efficacy (Chandran et al., 2015; Istifli et al., 2021). Therefore, prior knowledge of the interactions of hit molecules with the protein network of the host organism may help to reveal possible side effects or novel therapeutic effects of these molecules. In this study, the targets-components analysis of A7G and L7G was performed by selecting the target organism as '*Homo sapiens*' through the STITCH (http://stitch.embl.de/) public database.

3. Results and discussion

The molecular docking calculation results of A7G with AChE, BChE, APP, and Aβ peptide are demonstrated in Table 1 and Figures 2 and 5. A7G formed 3 H-bonds with Tyr62, Gln63, and His201, a π-π stacked interaction with Trp59, an unfavorable acceptor-acceptor interaction with Glu233, and a small number of van der Waals interactions in the catalytic cavity of AChE (Figure 5A).

Table 1. Free energy of binding and calculated inhibition constants of apigenin-7-glucoside, luteolin-7-glucoside and rivastigmine, a dual-inhibitor of acetylcholinesterase (AChE) and butyrylcholinesterase (BChE), against Alzheimer's disease-related proteins

No	Compound	Free energy of binding (kcal/mol)				Calculated inhibition constant (μM)			
		AChE	BChE	APP[1]	Aβ[2]	AChE	BChE	APP	Aβ
1	Apigenin-7-glucoside	-9.42	-9.60	-6.10	-6.0	0.180	0.091	33.78	39.99
2	Luteolin-7-glucoside	-9.30	-9.90	-6.30	-6.10	0.152	0.050	24.10	33.78
3	Rivastigmine*	-6.50	-6.90	-	-	17.20	8.76	-	-

* The binding free energy values obtained from the docking calculations of rivastigmine with AChE and BChE were used as positive controls.
[1] Amyloid precursor protein
[2] Amyloid-beta peptide

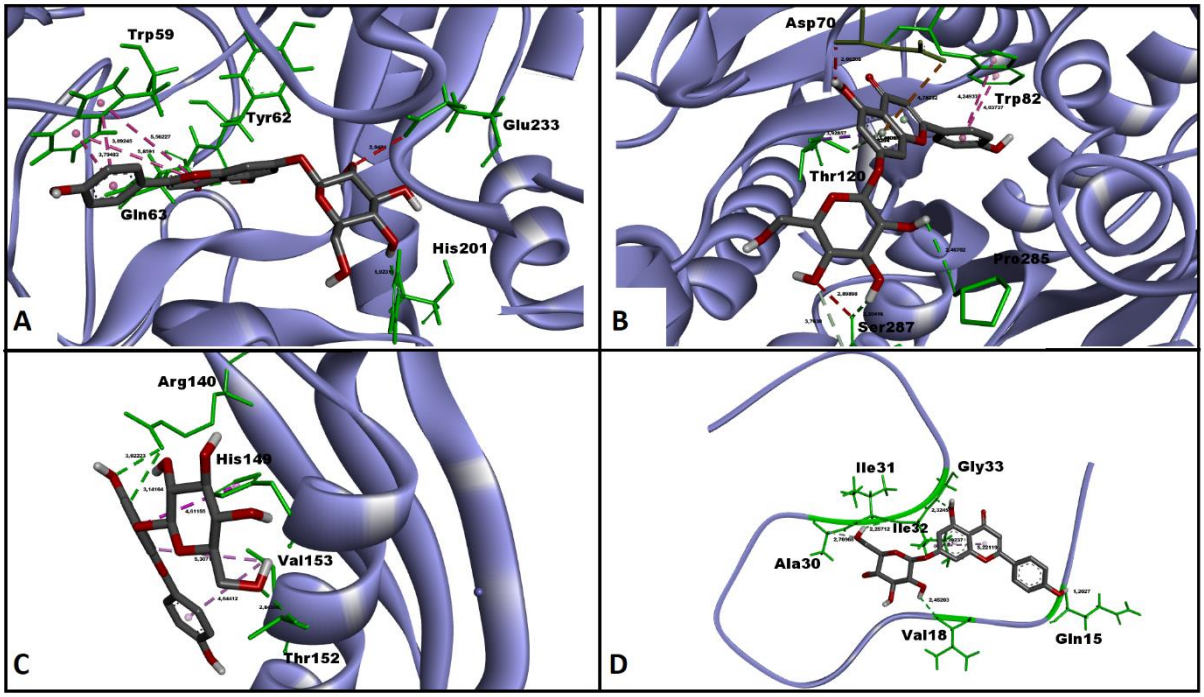

Figure 2. Figure 2. Top-ranked conformations of apigenin-7-glucoside (A7G) (A- Human AChE, B- Human BChE, C- Amyloid precursor protein [APP], D- Beta-amyloid [Aβ] peptide

The calculated free energy of binding of A7G with AChE is highly favorable (-9.42 kcal/mol; Ki=0.180 μM) (Table 1), and the top-ranked pose of A7G within the catalytic pocket of AChE is demonstrated in Figure 2A. A7G formed 3 H-bonds with Pro285, Ser287, a π-anion interaction with Asp70, two pi-donor hydrogen bonds with Thr120, a π-π stacked interaction with Trp82, and two unfavorable donor-donor and acceptor-acceptor interactions with Asp70 of BChE. In addition, A7G engaged in many van der Waals interactions in the catalytic cavity of BChE (Figure 5B). The calculated free energy of binding of A7G with BChE is highly favorable (-9.60 kcal/mol; Ki=0.091 μM) (Table 1), and the top-ranked pose of A7G within the catalytic pocket of BChE is

demonstrated in Figure 2B. The interactions of A7G within the catalytic pocket of APP included 3 H-bonds with Arg140 and Thr152, a π-π T-shaped, and a π-alkyl interaction with His149 and Val153, respectively, and a small number of van der Waals interactions in the copper-binding domain of APP (Figure 5C). The calculated free energy of binding of A7G with APP is moderately strong (-6.10 kcal/mol; Ki=33.78 µM) (Table 1), and the top-ranked pose of A7G within the copper-binding domain of APP is demonstrated in Figure 2C. A7G formed 3 H-bonds with Val18, Ile31, and Gly33, two π-alkyl interactions with Ile32, and an unfavorable donor-donor interaction with Gln15 of Aβ peptide (Figure 5D). It is noteworthy that the interaction of A7G with Gly33 is significant since this residue lies within the nucleation-dependent polymerization site of the Aβ peptide (Hsu et al., 2018). The calculated free energy of binding of A7G with Aβ peptide is moderately strong (-6.0 kcal/mol; Ki=39.99 µM) (Table 1), and the top-ranked pose of A7G within the nucleation-dependent polymerization site of Aβ peptide is demonstrated in Figure 2D.

The docking calculation results of L7G with AChE, BChE, APP, and Aβ peptide are demonstrated in Table 1 and Figures 3 and 5. L7G formed 7 H-bonds with Gln63, Arg195, Glu233, His299, and Asp300, three π-π stacked interactions with Trp59 and an unfavorable donor-donor interaction with Gln63 of AChE. The interactions of L7G with AChE also included many van der Waals interactions with surrounding residues (Figure 5E). The calculated free energy of binding of L7G with AChE is powerful (-9.30 kcal/mol; Ki=0.152 µM) (Table 1), and the top-ranked pose of L7G within the catalytic cavity of AChE is demonstrated in Figure 3A. L7G formed 8 H-bonds with Asn83, Thr120, Tyr128, Glu197, Thr284, Pro285, and Ser287, a π-anion interaction with Asp70 and a π-π stacked interaction with Trp82 of BChE. The interactions of L7G with BChE included many van der Waals contacts with surrounding residues (Figure 5F).

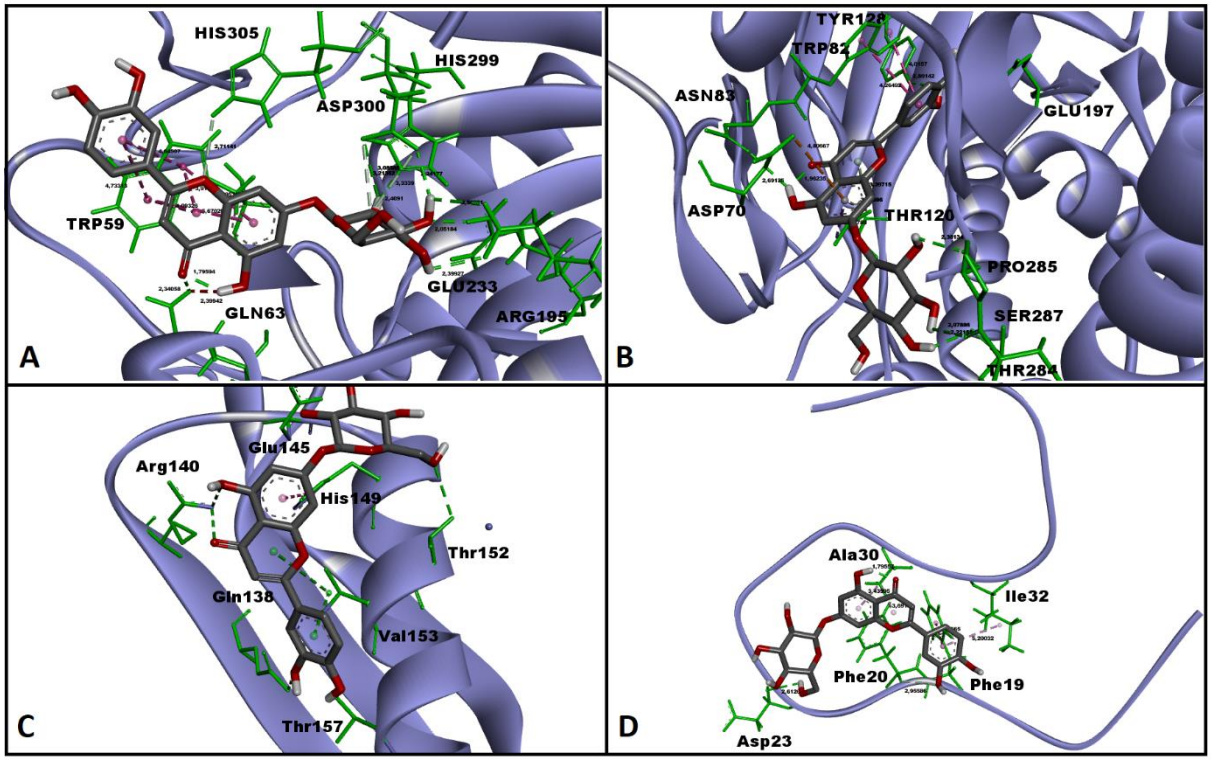

Figure 3. Top-ranked conformations of luteolin-7-glucoside (L7G) (A- Human AChE, B- Human BChE, C- Amyloid precursor protein [APP], D- Beta-amyloid [Aβ] peptide

The calculated free energy of binding of L7G with BChE is powerful (-9.90 kcal/mol; Ki=0.050 µM) (Table 1), and the top-ranked pose of L7G within the catalytic cavity of BChE is demonstrated in Figure 3B. The interactions of L7G with APP mainly included 7 H-bonds with Gln138, Arg140, Glu145, Thr152, and Thr157, a π-π T-shaped interaction with His149 and a π-alkyl interaction with Val153. However, the van der Waals contacts played a minor role in L7G's interactions with the APP (Figure 5G). The calculated free energy of binding of L7G with APP is moderately strong (-6.30 kcal/mol; Ki=24.20 µM) (Table 1), and the top-ranked pose of L7G within the copper-binding domain of APP is demonstrated in Figure 3C. Finally, L7G formed 2 H-bonds with Phe20 and Asp23, a π-π T-shaped interaction with Phe19 and three π-alkyl interactions with Ala30 and Ile32 of the nucleation-dependent polymerization site of the Aβ peptide. Van der Waals contacts also played a role in the interaction of L7G with the Aβ peptide (Figure 5H). The calculated free energy of binding of L7G with Aβ peptide is moderately strong (-6.10 kcal/mol; Ki=33.78 µM) (Table 1), and the top-ranked pose of L7G within the polymerization site of Aβ peptide is demonstrated in Figure 3D. Since Asp23 (D23) is significant for the sigmoidal aggregation kinetics of Aβ peptide, the hydrogen bond interaction between L7G and Asp23 is of utmost importance (Hsu et al., 2018).

In this study, the binding free energy and inhibition constant of rivastigmine against AChE and BChE were used as a positive control group to compare A7G and L7G interactions with these two enzymes. The docking calculation results of rivastigmine with AChE and BChE can be seen in Table 1 and Figure 5. Rivastigmine formed 3 H-bonds with Gln63, Glu233, and Asp300, two π-sigma interactions with Trp59 and Tyr62, a π-π stacked interaction with Tyr62 and two π-alkyl interactions with Leu165 and His299 of AChE. A certain number of van der Waals interactions also played a role in the rivastigmine-AChE interaction (Figure 5I). The calculated free energy of binding of rivastigmine with AChE is strong (-6.50

kcal/mol; Ki=17.20 µM) (Table 1), and the top-ranked pose of rivastigmine within the catalytic cavity of AChE is demonstrated in Figure 4A.

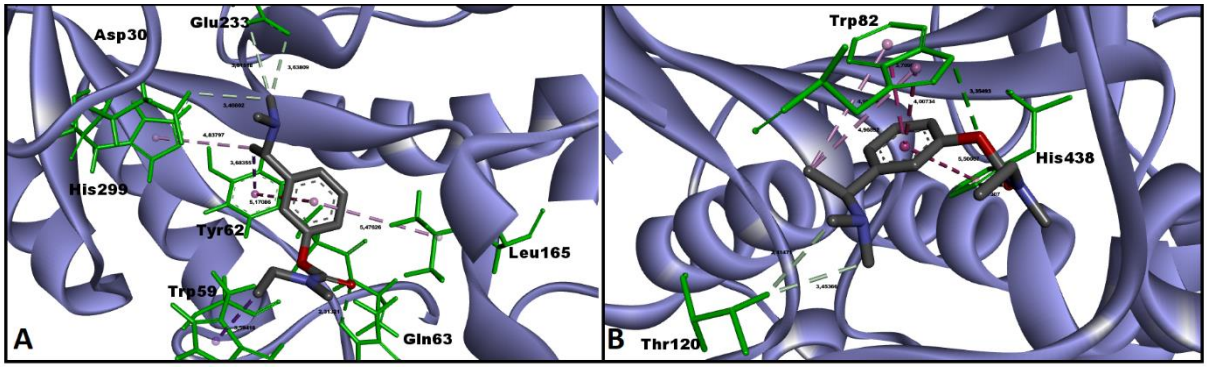

Figure 4. Top-ranked conformations of rivastigmine A- Human AChE, B- Human BChE

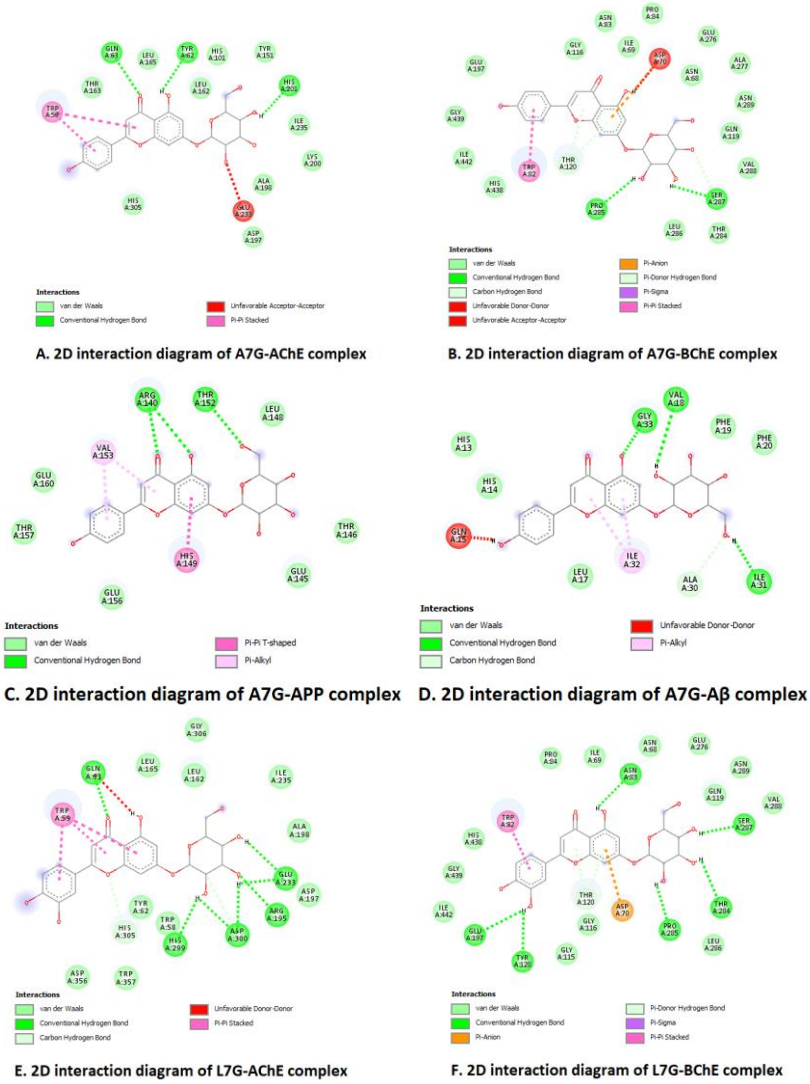

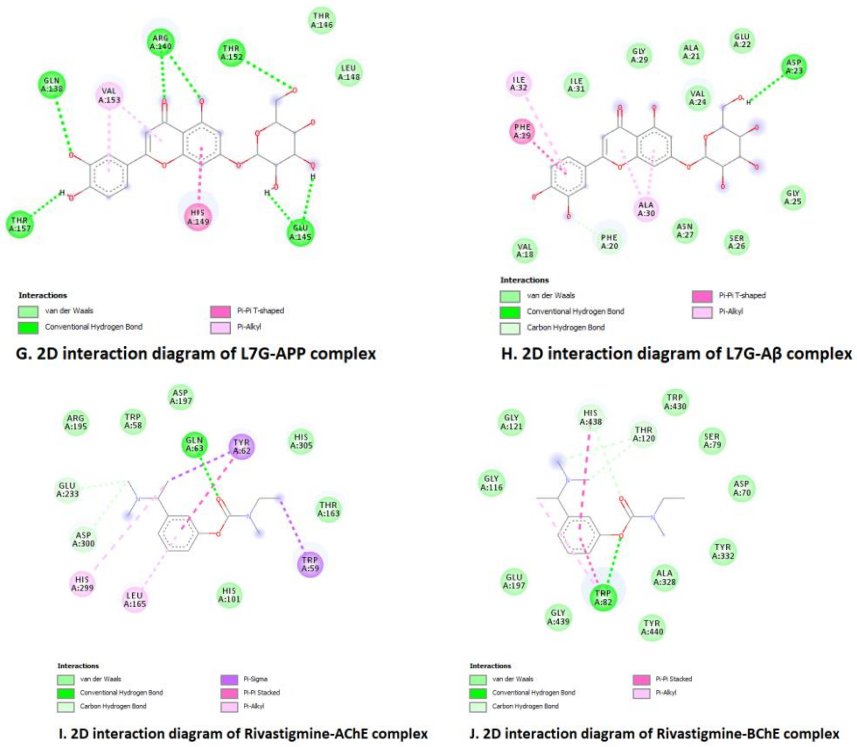

Figure 5. 2D interaction diagrams of the molecular interactions of apigenin-7-glucoside, luteolin-7-glucoside, and rivastigmine with their receptors in molecular docking simulations. A, B, C, D. Apigenin-7-glucoside; E, F, G, H. Luteolin-7-glucoside; I, J. rivastigmine

In the case of BChE, rivastigmine formed 4 H-bonds with Trp82, Thr120, and His438, two π-π stacked interactions with Trp82 and His438 and a π-alkyl interaction with Trp82. It can also be said that the effect of van der Waals contacts on the rivastigmine-BChE interaction is moderately strong (Figure 5J). The calculated free energy of binding of rivastigmine with BChE is also strong (-6.90 kcal/mol; Ki=8.76 μM) (Table 1), and the top-ranked pose of rivastigmine within the catalytic cavity of BChE is demonstrated in Figure 4B. The constant inhibition values obtained from the docking simulations of rivastigmine against AChE and BChE (17.20 μM for AChE; 8.76 μM for BChE) are in good agreement with the experimental IC_{50} values of the same ligand against both enzymes. It has been reported that the human AChE IC_{50} value of rivastigmine is 6.33 μM, and the human BChE IC_{50} value is 0.803 μM at the end of a 40-minute incubation period (Dighe et al., 2016).

Table 2. Drug-likeness properties of apigenin-7-glucoside and luteolin-7-glucoside

No	Compound	Number of rotatable bonds	TPSA[1]	Consensus Log P	Log S (ESOL[2])	Drug likeness (Lipinski's rule of five)
1	Apigenin-7-glucoside	4	170.05	0.55	-3.78	Yes; 1 violation: NH or OH>5
2	Luteolin-7-glucoside	4	190.28	0.16	-3.65	No; 2 violations: N or O > 10, NH or OH>5

[1] TPSA: Topological polar surface area (Å²)
[2] ESOL: Estimated aqueous solubility [(Insoluble < -10 < Poorly < -6 < Moderately < -4 < Soluble < -2 Very < 0 < Highly), according to Delaney, J.S. (2004)].
Data source: http://www.swissadme.ch/index.php

Drug-likeness, ADMET, and intracellular target profiles of A7G and L7G are given in Tables 2, 3, and Figure 6, respectively. Except for L7G, A7G was determined to obey Lipinski's rule of five. L7G violates this rule because it has N or O > 10 and NH or OH > 5 (Table 2). ADMET data of A7G and L7G are presented in Table 3.

Table 3. ADMET profiles of apigenin-7-glucoside and luteolin-7-glucoside

No	Compound	BBB permeation[1,*]	P-gp substrate[2,*]	CYP inhibition[3,*]	AMES Toxicity[4]	Hepatotoxicity[4]	LD_{50} in rat (mol/kg)[4]
1	Apigenin-7-glucoside	No	Yes	No	No	No	2.595
2	Luteolin-7-glucoside	No	Yes	No	No	No	2.547

[1] BBB: Blood Brain Barrier
[2] P-gp: P-glycoprotein substrate
[3] CYP: Cytochrome P
[4] http://biosig.unimelb.edu.au/pkcsm/prediction
[*] http://www.swissadme.ch/index.php

According to ADMET profiles, A7G and L7G cannot cross the blood-brain barrier (BBB) and are substrates of p-glycoprotein (P-gp); however, both compounds do not show CYP inhibition, AMES toxicity, and hepatotoxicity, and their acute toxicity potency (LD_{50}) is not high in rats (Table 3). The intracellular target of A7G is depicted in Figure 6A. According to the search by the SwissTarget online tool,

the intracellular targets of A7G most frequently include various enzymes, kinases, and family A G protein-coupled receptors. However, results from the same tool show that A7G is unlikely to have a positive/negative interaction on these targets (p <= 0.432) (Figure 6A). Intracellular targets of L7G, similar to A7G, most commonly include kinases, various enzymes, and family A G protein-coupled receptors. However, statistical analysis performed by the same tool indicates that L7G is less likely to have a positive/negative interaction on these targets (*p* <= 0.430) (Figure 6B).

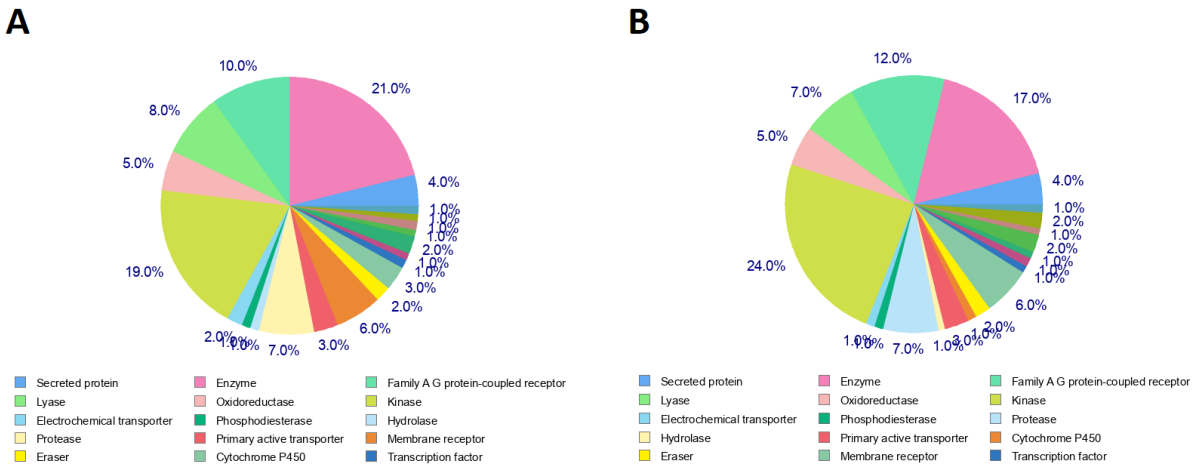

Figure 6. Intracellular target predictions of apigenin-7-glucoside and luteolin-7-glucoside

The STITCH platform was used to predict putative targets of A7G and L7G in the human proteome. Before mapping target-component interactions, the minimum required interaction score was set to a high confidence score which was ≥ 0.7. A high confidence score indicates a strong interaction between hit compounds and protein(s). According to the targets-components interaction network in Figure 7, it can be stated that A7G (cosmosiin) interacts directly with ADIPOQ and SLC2A4 proteins, while L7G directly interacts with MTRR, POR, HMOX1, NOS1, NOS2 and NOS3 proteins. Thus, the direct interactions of A7G and L7G with different proteins have been mapped (Figure 7).

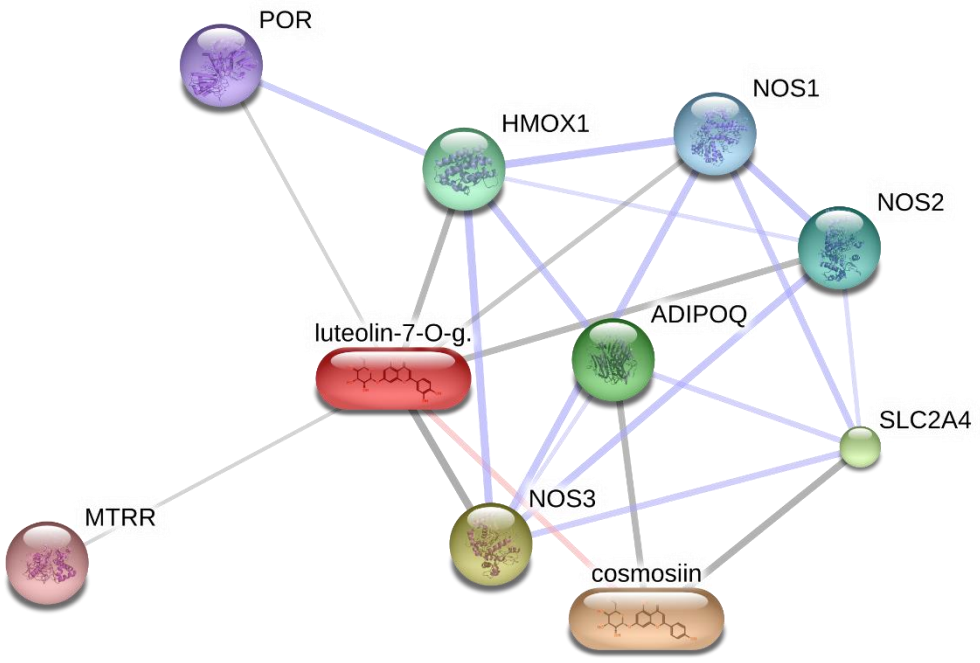

Figure 7. Targets-components analysis (chemical-protein interactions) of apigenin-7-glucoside (cosmos in) and luteolin-7-glucoside performed via the STITCH platform (http://stitch.embl.de)

So far, no drug discovery study was found targeting AChE, BChE, APP, and Aβ simultaneously involved in the etiology of AD. Therefore, this present study is the first to investigate the potential of A7G and L7G as drug candidates in the rational treatment of AD using a structure-based drug design approach. In this study, the binding affinity of A7G and L7G against AChE and BChE was found to be considerably higher than that of rivastigmine, a dual inhibitor of both enzymes (Table 1). With these properties, A7G and L7G can be recommended as natural AChE and BChE inhibitors. Consistent with the findings of this study, a chemical composition, and molecular

docking analysis study reported that the dominant flavonoid glycosides (A7G and L7G) in two *Onosma* species showed very high binding affinities for AChE and BChE (Istifli, 2021). At the molecular level, A7G exerts its ameliorative effect on cognitive impairment by inhibiting COX-2 and iNOS enzymes and may slow down the cognitive regression in AD disease (Patil et al., 2003).
Interestingly, these reported protein targets of A7G are not similar to those predicted by the STITCH server (ADIPOQ and SLC2A4) (Figure 7) and have no relation in the human proteome. Thus, A7G is likely to have more targets in the human proteome than is known in the AD-related literature. It has been shown in an experimental and molecular modeling study that L7G has the potential to inhibit AChE and BChE similar to A7G (Istifli, 2021). Since inducible nitric oxide synthase (iNOS) enzymes involved in inflammation are among the enzymes targeted by L7G in the human proteome (Figure 7), L7G may also show its positive effect in AD by blocking iNOS enzymes. The genetic ablation of iNOS protects against AD-like disease in mice supports this hypothesis (Nathan et al., 2005).

In this study, A7G and L7G showed a moderately favorable binding affinity against the APP and Aβ peptide (Table 1). No experimental or docking studies of A7G and L7G against APP and Aβ peptides were found in the literature. However, it has been reported that the non-glycosidic form of A7G, apigenin, reduces the phosphorylation of ERK1/2 and CREB proteins (Salehi et al., 2019; Zhao et al., 2013), while the non-glycosidic form of L7G, luteolin, inhibits the N-acetyl-alpha-galactosaminyltransferase (ppGalNAc-T) enzyme thereby slowing down the amyloidogenic process (Liu et al., 2017). These reported experimental results are in agreement with the results we obtained from the docking analyses. It has been reported that flavonoids are hydrolyzed and then glucuronidated in the gut (Tundis et al., 2012). Glucuronidation, in turn, results in much higher water solubility; therefore, glycosidic forms are likely to reach the central nervous system. According to the ADMET predictions (Table 3) we employed, A7G and L7G were both found unable to pass the blood-brain barrier; however, this estimation via the SwissADME web tool is based on a machine-learning algorithm, and the cross-validation accuracy of this technique has been reported to be 88% (Daina et al., 2019b). On the other hand, experimental results confirmed that A7G and L7G could, hopefully, cross the blood-brain barrier (Qin et al., 2019; Salehi et al., 2019).

4. Conclusions

This study determined that in molecular docking simulations, A7G and L7G showed high affinity against AChE, BChE, APP, and Aβ peptides. Compared with rivastigmine, A7G and L7G exhibit a highly favorable binding free energy against AChE and BChE and possess the potential of being hit molecules. Considering the drug-likeness, ADMET, and intracellular targets, A7G and L7G have the physicochemical properties that should be found in a drug (although L7G violates Lipinski's rule of 5 at two points), they do not show significant toxicity. They do not have the potential to inhibit intracellular enzymes or proteins significantly. Both compounds may have the potential to positively change the course of AD by showing an inhibitory effect on enzymes (ADIPOQ, NOS1, NOS2, and NOS3) that play essential roles in cellular inflammation processes. However, the possible interaction of L7G with POR (cytochrome P450 oxidoreductase) could be problematic and may influence the patient's response to particular drugs. Although the affinity of A7G and L7G towards APP and Aβ is not highly favorable, molecular modification may increase the affinity of both drugs for these essential AD-related proteins. Further experimental studies will elucidate the actual applicability of these two ligands in the multi-targeted treatment of AD in more detail.

Acknowledgments

None.

Conflict of Interest

The authors confirm that there are no known conflicts of interest.

CRediT authorship contribution statement

Erman Salih Istifli: Conceptualization, Data curation, Formal analysis, Investigation, Methodology, Software, Visualization, Writing, Review & Editing
Cengiz Sarikurkcu: Data curation, Investigation, Software, Methodology, Review & Editing

ORCID IDs of the Authors

E. S. Istifli: 0000-0003-2189-0703
C. Sarikurkcu: 0000-0001-5094-2520

References

Airoldi, C., La Ferla, B., D'Orazio, G., Ciaramelli, C., Palmioli, A., 2018. Flavonoids in the treatment of Alzheimer's and other neurodegenerative diseases. *Current medicinal chemistry*, 25(27), 3228-3246.
Ali, M.Y., Jannat, S., Edraki, N., Das, S., Chang, W.K., Kim, H.C., Park, S.K., Chang, M.S., 2019. Flavanone glycosides inhibit β-site amyloid precursor protein cleaving enzyme 1 and cholinesterase and reduce Aβ aggregation in the amyloidogenic pathway. *Chemico-biological interactions*, 309, 108707.
Álvarez Rojas, A., Moreno Mauro, R.D., Garrido, J., 1996. Acetylcholinesterase Accelerates Assembly of Amyloid-B-Peptides Into Alzheimer's Fibrils: Possible Role of the Peripheral Site of the Enzyme. *Neuron*, 16(4), 881-891.
Anderson, J.P., Chen, Y., Kim, K.S., Robakis, N.K., 1992. An alternative secretase cleavage produces soluble Alzheimer amyloid precursor protein containing a potentially amyloidogenic sequence. *Journal of neurochemistry*, 59(6), 2328-2331.
Burns, A., Iliffe, S., 2009. Alzheimer's disease. BMJ 338, b158.
Carvajal, F.J., Inestrosa, N.C., 2011. Interactions of AChE with Aβ aggregates in Alzheimer's brain: therapeutic relevance of IDN 5706. *Frontiers in Molecular Neuroscience*, 4, 19.
Chandran, U., Mehendale, N., Tillu, G., Patwardhan, B., 2015. Network Pharmacology of Ayurveda Formulation Triphala with Special Reference to Anti-Cancer Property. *Comb Chem High Throughput Screen*, 18(9), 846-854.
Daina, A., Michielin, O., Zoete, V., 2019a. SwissTargetPrediction: updated data and new features for efficient prediction of protein targets of small molecules. *Nucleic Acids Research*, 47(W1), W357-W364.
Daina, A., Michielin, O., Zoete, V., 2019b. SwissTargetPrediction: updated data and new features for efficient prediction of protein targets of small molecules. *Nucleic Acids Res*, 47(W1), W357-W364.
Darvesh, S., Cash, M.K., Reid, G.A., Martin, E., Mitnitski, A., Geula, C., 2012. Butyrylcholinesterase is associated with β-amyloid plaques in the transgenic APPSWE/PSEN1dE9 mouse model of Alzheimer disease. *Journal of Neuropathology & Experimental Neurology*, 71(1), 2-14.
Dighe, S.N., Deora, G.S., De la Mora, E., Nachon, F., Chan, S., Parat, M.O., Brazzolotto, X., Ross, B.P., 2016. Discovery and Structure-Activity Relationships of a Highly Selective Butyrylcholinesterase Inhibitor by Structure-Based Virtual Screening. *J Med Chem*, 59(16), 7683-7689.
Dinamarca, M.C., Sagal, J.P., Quintanilla, R.A., Godoy, J.A., Arrázola, M.S., Inestrosa, N.C., 2010. Amyloid-β-Acetylcholinesterase complexes potentiate neurodegenerative changes induced by the Aβ peptide. Implications for the pathogenesis of Alzheimer's disease. *Molecular neurodegeneration*, 5(1), 1-15.
Ferri, C.P., Prince, M., Brayne, C., Brodaty, H., Fratiglioni, L., Ganguli, M., Hall, K., Hasegawa, K., Hendrie, H., Huang, Y., 2005. Global prevalence of dementia: a Delphi consensus study. *The lancet*, 366(9503), 2112-2117.
Francis, P.T., Palmer, A.M., Snape, M., Wilcock, G.K., 1999. The cholinergic hypothesis of Alzheimer's disease: a review of progress. *Journal of Neurology, Neurosurgery & Psychiatry*, 66(2), 137-147.
Gabuzda, D., Busciglio, J., Chen, L.B., Matsudaira, P., Yankner, B.A., 1994. Inhibition of energy metabolism alters the processing of amyloid precursor protein and induces a potentially amyloidogenic derivative. *Journal of Biological Chemistry*, 269(18), 13623-13628.
Greig, N.H., Lahiri, D.K., Sambamurti, K., 2002. Butyrylcholinesterase: an important new target in Alzheimer's disease therapy. *International Psychogeriatrics*, 14(S1), 77-91.
Guzzi, C., Colombo, L., Luigi, A.D., Salmona, M., Nicotra, F., Airoldi, C., 2017. Flavonoids and Their Glycosides as Anti-amyloidogenic Compounds: Aβ1–42 Interaction Studies to Gain New Insights into Their Potential for Alzheimer's Disease Prevention and Therapy. *Chemistry–An Asian Journal*, 12(1), 67-75.

Haass, C., Schlossmacher, M.G., Hung, A.Y., Vigo-Pelfrey, C., Mellon, A., Ostaszewski, B.L., Lieberburg, I., Koo, E.H., Schenk, D., Teplow, D.B., 1992. Amyloid β-peptide is produced by cultured cells during normal metabolism. *Nature*, 359(6393), 322-325.

Hanwell, M.D., Curtis, D.E., Lonie, D.C., Vandermeersch, T., Zurek, E., Hutchison, G.R., 2012. Avogadro: an open-source molecular builder and visualization tool. *Journal of Cheminformatics*, 4, 17.

Hardy, J., Allsop, D., 1991. Amyloid deposition as the central event in the aetiology of Alzheimer's disease. *Trends in pharmacological sciences*, 12, 383-388.

Hsu, F., Park, G., Guo, Z., 2018. Key residues for the formation of Aβ42 amyloid fibrils. *ACS omega*, 3(7), 8401-8407.

Inestrosa, N.C., Sagal, J.P., Colombres, M., 2005. Acetylcholinesterase interaction with Alzheimer amyloid β. *Alzheimer's Disease*, 38, 299-317.

Istifli, E.S., 2021. Chemical Composition, Antioxidant and Enzyme Inhibitory Activities of Onosma bourgaei and Onosma trachytricha and in Silico Molecular Docking Analysis of Dominant Compounds. *Molecules*, 26(10), 2981.

Istifli, E.S., Sihoglu Tepe, A., Sarikurkcu, C., Tepe, B., 2021. Investigation of molecular interactions between some hydroxybenzoic and hydroxycinnamic acids and the receptor binding site (RBD) of 2019-nCoV spike protein and host proteases [transmembrane protease, serin 2 (TMPRSS2), cathepsin B and cathepsin L] by in silico analysis. *International Journal of Secondary Metabolite*, 8(3), 246-271.

Li, B., Stribley, J.A., Ticu, A., Xie, W., Schopfer, L.M., Hammond, P., Brimijoin, S., Hinrichs, S.H., Lockridge, O., 2000. Abundant tissue butyrylcholinesterase and its possible function in the acetylcholinesterase knockout mouse. *Journal of neurochemistry*, 75(3), 1320-1331.

Li, H., Robertson, A.D., Jensen, J.H., 2005. Very fast empirical prediction and rationalization of protein pKa values. *Proteins*, 61(4), 704-721.

Liu, F., Xu, K., Xu, Z., de Las Rivas, M., Wang, C., Li, X., Lu, J., Zhou, Y., Delso, I., Merino, P., 2017. The small molecule luteolin inhibits N-acetyl-α-galactosaminyltransferases and reduces mucin-type O-glycosylation of amyloid precursor protein. *Journal of Biological Chemistry*, 292(52), 21304-21319.

Nathan, C., Calingasan, N., Nezezon, J., Ding, A., Lucia, M.S., La Perle, K., Fuortes, M., Lin, M., Ehrt, S., Kwon, N.S., 2005. Protection from Alzheimer's-like disease in the mouse by genetic ablation of inducible nitric oxide synthase. *Journal of Experimental Medicine*, 202(9), 1163-1169.

O'Boyle, N.M., Banck, M., James, C.A., Morley, C., Vandermeersch, T., Hutchison, G.R., 2011. Open Babel: An open chemical toolbox. *Journal of Cheminformatics*, 3, 33.

Patil, C.S., Singh, V.P., Satyanarayan, P., Jain, N.K., Singh, A., Kulkarni, S.K., 2003. Protective effect of flavonoids against aging-and lipopolysaccharide-induced cognitive impairment in mice. *Pharmacology*, 69(2), 59-67.

Pires, D.E., Blundell, T.L., Ascher, D.B., 2015. pkCSM: Predicting Small-Molecule Pharmacokinetic and Toxicity Properties Using Graph-Based Signatures. *Journal of Medicinal Chemistry*, 58(9), 4066-4072.

Qin, L., Chen, Z., Yang, L., Shi, H., Wu, H., Zhang, B., Zhang, W., Xu, Q., Huang, F., Wu, X., 2019. Luteolin-7-O-glucoside protects dopaminergic neurons by activating estrogen-receptor-mediated signaling pathway in MPTP-induced mice. *Toxicology*, 426, 152256.

Salehi, B., Venditti, A., Sharifi-Rad, M., Kregiel, D., Sharifi-Rad, J., Durazzo, A., Lucarini, M., Santini, A., Souto, E.B., Novellino, E., Antolak, H., Azzini, E., Setzer, W.N., Martins, N., 2019. The Therapeutic Potential of Apigenin. *International Journal of Molecular Sciences*, 20(6).

Seubert, P., Oltersdorf, T., Lee, M.G., Barbour, R., Blomquist, C., Davis, D.L., Bryant, K., Fritz, L.C., Galasko, D., Thal, L.J., 1993. Secretion of β-amyloid precursor protein cleaved at the amino terminus of the β-amyloid peptide. *Nature*, 361(6409), 260-263.

Seubert, P., Vigo-Pelfrey, C., Esch, F., Lee, M., Dovey, H., Davis, D., Sinha, S., Schiossmacher, M., Whaley, J., Swindlehurst, C., 1992. Isolation and quantification of soluble Alzheimer's β-peptide from biological fluids. *Nature*, 359(6393), 325-327.

Spoerri, L., Vella, L.J., Pham, C.L., Barnham, K.J., Cappai, R., 2012. The amyloid precursor protein copper binding domain histidine residues 149 and 151 mediate APP stability and metabolism. *Journal of Biological Chemistry*, 287(32), 26840-26853.

Sun, X., Chen, W.-D., Wang, Y.-D., 2015. β-Amyloid: the key peptide in the pathogenesis of Alzheimer's disease. *Frontiers in Pharmacology*, 6, 221.

Trott, O., Olson, A.J., 2010. AutoDock Vina: improving the speed and accuracy of docking with a new scoring function, efficient optimization, and multithreading. *Journal of Computational Chemistry*, 31(2), 455-461.

Tundis, R., Bonesi, M., Menichini, F., Loizzo, M.R., Conforti, F., Statti, G., Pirisi, F.M., Menichini, F., 2012. Antioxidant and anti-cholinesterase activity of Globularia meridionalis extracts and isolated constituents. *Natural product communications*, 7(8), 1934578X1200700814.

Uddin, M., Kabir, M., Niaz, K., Jeandet, P., Clément, C., Mathew, B., Rauf, A., Rengasamy, K.R., Sobarzo-Sánchez, E., Ashraf, G.M., 2020. Molecular insight into the therapeutic promise of flavonoids against Alzheimer's disease. *Molecules*, 25(6), 1267.

Valdes-Tresanco, M.S., Valdes-Tresanco, M.E., Valiente, P.A., Moreno, E., 2020. AMDock: a versatile graphical tool for assisting molecular docking with Autodock Vina and Autodock4. *Biology Direct*, 15(1), 12.

Zhao, L., Wang, J.-L., Liu, R., Li, X.-X., Li, J.-F., Zhang, L., 2013. Neuroprotective, anti-amyloidogenic and neurotrophic effects of apigenin in an Alzheimer's disease mouse model. *Molecules*, 18(8), 9949-9965.